

Adaptive Spatial Steganography Based on Probability-Controlled Adversarial Examples

Sai Ma, Qingxiao Guan, Xianfeng Zhao, and Yaqi Liu

Abstract—Deep learning model is vulnerable to adversarial attack, which generates special input sample to the deep learning model that can make the model misclassify the sample. Besides deep learning model, adversarial attack is also effective to feature-based machine learning model. In this paper, we discuss the application of adversarial attack for improving the capability to resist steganalysis of steganographic schemes. We apply the steganalytic neural network as the adversarial generator. Our goal is to improve the performance of typical spatial adaptive steganography towards the steganalysis of rich model feature and neural network. The adversarial method can be combined with adaptive steganography by controlling the flipping directions of pixels following the gradient map. The steganographic adversarial example can make itself “seems like” innocent cover towards steganalyzer. However, the generated steganographic adversarial examples are only effective to deceive the steganalyzer trained with non-adversarial examples. When facing the steganalyzer trained with adversarial examples, they can be easily detected with a low detecting error rate. The adversarial method makes the generated stego image more distinguishable from the cover image. To improve this situation, we adjust the method to calculate the gradient map by modifying the probability vector of softmax layer to a particular vector rather than modifying the category vector. Therefore, the generated adversarial example is controlled by probability output of softmax. With the adjustment, the adversarial scheme performs better than the typical adaptive steganography. We develop an practical adversarial steganographic method with double-layered STC. The experiment proves its effectiveness on rich model and neural network.

Index Terms—steganography, adversarial attack, deep learning, steganalysis.

I. INTRODUCTION

NOWADAYS, the mainstream scheme of steganography is distortion-minimizing steganographic scheme. The scheme is also named as adaptive steganographic scheme. The scheme consists of two phases. The first phase is assigning a cost value to every element of cover object. The assigned cost value reflects the impact of changing the corresponding element. The sum of the cost values of changed elements is stego distortion. The mission of the scheme is to minimize the distortion. The second phase is embedding the secret message in the cover object. The embedding process is changing the elements of cover object with widely accepted efficient coding method named STC(Syndrome-Trellis Code)[1]. As STC has a good performance that can approximate the rate-distortion bound, the researchers pay more attentions on improving the security of distortion function.

The purpose to define the steganographic distortion function is to evaluate the statistical impact of steganographic modification. As digital image is a kind of data that has high dimension and complicated correlation, designing the distortion function is a challenging work. Many distortion functions follows heuristic principles. Intuitively, the most important principle of the distortion function is that the complicated area of image should have more stego modifications than the simple area. The reason is that it is hard for the image steganalyzer to capture the abnormal pattern of complicated area.

The typical distortion functions are derived from the local difference or the high-pass residual of images. The first distortion function is HUGO[2]. It calculates the pixel’s stego modification cost via the differences of the pixel and its local neighbors. WOW[3] is another distortion function. It is constructed by wavelet filters. WOW captures the perturbation in wavelet domain. UNIWARD[4] is similar with WOW, which is also based on wavelet. Comparing with former methods, UNIWARD can be applied in all kinds of scenario: spatial(S-UNIWARD), JPEG(J-UNIWARD), and side-informed(SI-UNIWARD). In 2014, Li et al. proposed HILL[5], which further improves WOW. HILL applies the spreading rule [6] that makes the pixels’ cost values gather the embedding changes in the complex area of the image. HILL has a better performance than WOW and S-UNIWARD.

Besides heuristic design principle of distortion function, there is another design principle based on local statistical model. In this principle, the distortion is derived by likelihood ratio test. The distortion functions following this principle are MG[7] and MIPOD[8]. Especially, MIPOD relates the detectability of the steganalyzer and the distortion function. Also, with spreading rule, MIPOD has the similar performance of HILL.

The distortion function is important for steganographic security. The embedding rule is also important for improving the security. Embedding the secret message following specific pattern can also resist the detection steganalyzer. One prevailing principle is SMD(Synchronizing Modification Direction). In SMD, the mutual effects of local modifications are taken into account. Therefore, the embedding modifications of each pixel is dependent, so to avoid introducing particular patterns that can be captured by steganalyzer. The typical SMD methods include: CMD[9], Synch[10], and DeJoin[11].

As rich-model-based steganalytic method has outstanding performance, researchers start to explore the deep-learning-based steganalytic method. The first attempt is [12], but its performance cannot reach SRM[13]. In 2015, Qian et al. proposed first deep-learning-based steganalytic method

The authors are with Institute of Information Engineering, Chinese Academy of Sciences, Beijing 100093, China. (e-mail: masai, guanqingxiao, zhaoxianfeng, liuyaqi@iie.ac.cn)

named GNCNN[14], which has comparable performance to rich model feature. In 2016, Xu et al. proposed XuNet[15], whose performance is better than rich model. In 2017, Ye et al. proposed YeNet[16]. YeNet applies selection-channel method and well-designed activation function named TLU for steganalysis. Comparing with rich model, deep-learning-based methods have diversity in implementation and higher accuracy.

Besides steganalysis, GAN(Generative Adversarial Network) based steganography is also proposed. The first GAN based steganography is [17]. [17] is generating cover image from noise via GAN. Another GAN based steganography[18] is construct distortion function automatically via GAN, which can approximate the performance of typical adaptive steganography. The GAN based steganographic schemes still needs improvements to reach the state of the art.

In 2013, Szegedy et al. [19] reported that deep model is vulnerable to adversarial example. Adversarial examples is the input data generated from raw data for deceiving the classifier and it only has slight difference with the raw data. For example, in image classification task, the classifier is a optimized neural network, adversarial example can be misclassified even through the difference between adversarial example and raw data cannot be recognized by eyes. Goodfellow et al. gave an explanation with linear perspective[20]. The explanation yields an effective method to generate adversarial example named FGSM(Fast Gradient Sign Method). FGSM generates the adversarial perturbation from gradient signal and the adversarial example is classified to a wrong category with a high confidence.

Adversarial attack to the neural network indicates that the network model can be a generator to produce adversarial examples. As proposed in [19][20], the adversarial attack is effective to various types of classifiers, which means it is not restricted to neural network. Therefore, adversarial examples can be exploited to attack various kind of steganalyzers. We can enhance the security of steganographic algorithms with the help of adversarial attack.

In this paper, we propose a new framework that applies adversarial method in steganography. As adversarial example is derived from gradient map of neural network, we apply steganalytic neural network model as the generator to produce steganographic adversarial example. We apply two kinds of steganalyzers to test the proposed method, which are rich model and neural network. The steganographic adversarial example carries the secret message and is generated with adversarial method. Specifically, we modify the image pixel following the adversarial gradient map while embedding. Here the adversarial gradient map is the matrix generated from neural network model and has the same size with the cover image. Each element of adversarial gradient map is the gradient value that make the steganalyzer tend to have a false classifying result. The proposed method can be a framework to utilize adversarial methods because it is not restricted to a particular distortion function or coding method. The framework can be applied to improve every existing adaptive steganographic methods. In this paper we demonstrate it with spatial methods.

Comparing with the typical adaptive steganographic schemes, the adversarial method has an advantage that it

can exploit the steganalyzer to enhance the security. The adversarial example decides the flipping direction of every changed pixels according to gradient map of steganalytic neural network automatically, but not following the heuristic principles. Except GAN-based methods, the former steganographic schemes cannot exploit characteristics of the steganalyzer directly to improve performance. Therefore the proposed adversarial method is meaningful to improve the steganographic security of existing methods.

In practice, we find that the simple transfer of adversarial method from computer vision to digital image steganography cannot enhance the security of steganographic method. The generated steganographic adversarial examples can only deceive the steganalyzer trained with non-adversarial examples. For the steganalyzer trained with adversarial examples, they can be easily detected. To solve the problem, we make an adaptation to the adversarial method that makes it suitable to the steganography. Specifically, we modify the output vector of softmax rather than the final output vector of category. We set softmax output to $[0.5, 0.5]$, which means that both the probability of cover and stego are 0.5. Therefore, the gradient map is generated from the most undistinguishable classifying result rather than making the classifying result tend to cover category. The generated steganographic adversarial example is probability-controlled, comparing with the adversarial examples generated by category-controlled. The experimental result proves that the adaptation is effective, and the proposed adversarial method can improve the security of steganographic algorithms for resisting the detection by the steganalyzer trained with adversarial examples. We propose a practical adversarial method on double-layered STC for spatial steganography by updating the cost value of $+1$ and -1 . The experiment shows that the proposed method can improve the steganographic security significantly. Comparing with the classical adaptive steganography, our method only needs a neural network model to generate a gradient map for the cover. Our method is practical to enhance the security of steganographic schemes.

The rest of paper is organized as follows. Section II introduces some basic conceptions of steganography, which are needed in the paper. Section III describes the adversarial attack in detail. Section IV discusses the application of adversarial method in steganography and available adaptation. Section V proposes a practical adversarial steganographic scheme based on double-layered STC. Section VI is experiment part. Section VII is conclusion.

II. PRELIMINARIES

In this paper, the image is spatial 8-bit gray-scale, so the dynamic range of a pixel value is $\{0, 1, \dots, 255\}$.

A. Distortion-minimizing framework

Distortion-minimizing steganography can be normalized to an optimization problem which is to find an optimal distribution on cover sequence and then to find an optimal modification pattern of the cover sequence.

The cover sequence is $\mathbf{x} = (x_1, x_2, \dots, x_i, \dots, x_n)$. The message sequence to be embedded into the cover is \mathbf{m} and its length is noted as $\|\mathbf{m}\|$. After embedding, the stego sequence is $\mathbf{y} = (y_1, y_2, \dots, y_i, \dots, y_n)$. Generally, the stego distortion of y is noted as $D(\mathbf{x}, \mathbf{y})$ and simply noted as $D(\mathbf{y})$. The probability that modifying \mathbf{x} to \mathbf{y} is noted as $\pi(\mathbf{x}, \mathbf{y})$ and simply noted as $\pi(\mathbf{y})$.

The optimal problem is described as: given a cover sequence \mathbf{x} and stego payload length $\|\mathbf{m}\|$, we need to find a optimal distribution $\pi(\mathbf{y})$ which has a minimal stego distortion.

$$\begin{aligned} & \arg \min_{\mathbf{y}} \sum_{\mathbf{y}} D(\mathbf{y}) \pi(\mathbf{y}) \\ & s.t. \sum_{\mathbf{y}} -\pi(\mathbf{y}) \log(\pi(\mathbf{y})) = \|\mathbf{m}\| \end{aligned} \quad (1)$$

With maximum entropy theory, we can get a close solution of (1):

$$\pi(\mathbf{y}) = \frac{1}{Z(\lambda)} \exp(-\lambda D(\mathbf{y})) \quad (2)$$

The distribution with this form is called Gibbs distribution. In (2), $Z(\lambda) = \sum_{\mathbf{y}} \exp(-\lambda D(\mathbf{y}))$, which is a partition function. λ is the parameter that can be determined with constraint condition.

If there is not any condition to limit (1), it is hard to get its numerical solution. To make the problem practical, there is an important assumption that stego modification to cover element is independent and does not affect other element. This assumption makes the distortion additive. The steganographic schemes under this assumption is also named as additive model. With the model, \mathbf{y} 's distortion can be converted into sum of elements' cost values and its probability can be decomposed into element-wise probabilities. In case of ± 1 embedding,

$$\begin{aligned} D(\mathbf{y}) &= \sum_{i=1, \dots, n; * \in \{+, -, 0\}} \pi_i^* \rho_i^* \\ \pi_i^* &= \frac{\exp(-\lambda \pi_i^*)}{\sum_{o \in \{+, -, 0\}} \exp(-\lambda \rho_i^o)} \end{aligned} \quad (3)$$

In (3), the superscripts of π_i and ρ_i represent the modification of +1, -1, and 0. It is clearly that $\rho_i^0 = 0$. With (3) we can compute the numerical results and simulate the optimal embedding.

In practical scenario, steganographer applies STC to approximately implement distortion-minimizing embedding. For typical ± 1 embedding, there is another assumption:

$$\rho_i^+ = \rho_i^- \quad (4)$$

Note that the assumption excludes the case that element is wet(value is saturated). The impact of +1 is the same with -1 under the assumption. In ± 1 simulation, the modification(+1 or -1) is chosen randomly. In ± 1 embedding, the modification is determined by secret message.

B. Steganographic security

The contemporary steganalysis is based on pattern reorganization. The task is a binary classification problem, which

is classifying the instance to cover image or stego image. Although the rich model steganalytic feature has good performance, it still has detection error. Therefore, researchers adopt detection error rate as a quantification to evaluate the performance of a steganographic method. The detection error P_E is:

$$P_E = \frac{1}{2}(P_{FA} + P_{MD}) \quad (5)$$

In (5), P_{FA} is probability of false alarm and P_{MD} is probability of missed detection.

The evaluation consists of two steps, which are training and testing. It should be emphasised that the both the training stego images and the testing stego images are generated via the steganographic method being evaluated. The result of evaluation, P_E , reflects the steganalyzer's ability to distinguish the the cover samples and stego samples.

P_E is an acknowledged performance metric for both steganalyzer and steganographic scheme. To steganographic scheme, it implies the capability to confuse the steganalyzer.

C. Synchronizing strategy

The additive model is based on the assumption (4), which does not consider the modification direction. In fact, the modification direction also affects the steganographic detectability. [9] [10] and [11] report the strategy that exploits the modification direction against detection. The strategy is named as synchronizing modification direction(SMD).

The rich model steganalytic feature is equipped with a batch of high-pass filters, which are selected with special local patterns. The feature is constructed with the high-order statistics of residuals obtained from the filtering. The rich model consists of multiple sub-models and each sub-model is build with a specific high-pass filter. The propose of this construction is to capture abnormal pattern introduced by the stego modification. On the contrary, the SMD's purpose is to avoid introducing the stego ± 1 modification pattern to neighborhood of each pixel. SMD encourages the adjacent stego modification to have the same direction.

Regardless of different implementation of SMD in [9], [10], and [11], they have the similar method to update cost values. Essentially, that is to make:

$$\rho^+ \neq \rho^- \quad (6)$$

With (6), modification direction can be controlled. One practical implementation of (6) is:

$$\begin{cases} \frac{1}{A} \rho^*, & \text{if encourage } *; \\ A \rho^*, & \text{if discourage } *. \end{cases} \quad (7)$$

In (17), $A > 1$ and $* \in \{-1, +1\}$. (17) satisfies (6). Therefore, the modification direction tends to the expected direction. As a pixel $x_i \in \{0, \dots, 255\}$, its minimum relative value is $1/256$. For contemporary steganalyzer, it is significant enough to detect the stego steganographic pattern in a digital image.

SMD strategy extends the distortion function to non-additive and receives good performance. However, the SMD-based method are all following heuristic principles.

III. ADVERSARIAL ATTACK

A. What is adversarial attack

In [19], Szegedy et al. report that the deep neural network can not correctly classify the instance which is added an imperceptible perturbation. This property is counter-intuitive because the neural network has high performance and seems to be robust to small perturbations. This kind of perturbations are non-random and intentionally constructed to maximize the classifying error. A well-trained neural network may get an arbitrary output when its input applies this kind of perturbation. We term the instance applying such perturbation "adversarial example".

Applying adversarial example for deceiving the classifier is named as "adversarial attack". Given a classifier based on neural network, the attacker can exploit adversarial example to make the classifier output a wrong result. In [19], the authors suggest that adversarial example is not a random artifact of neural network. Such fact implies that adversarial examples are robust to classifiers' parameters and structures. That is, the adversarial example generated from a neural network is also effective in deceiving other different networks or even feature-based classifiers. For the attacker, he needn't to get access to the inner detail of classifier to commit an adversarial attack, which is also known as "black-box attack". Therefore, the adversarial attack is generalized to various kinds of classifiers. With these advantages, attackers can use adversarial examples to attack various kinds of systems based on deep learning. This intriguing property of neural network has drawn attentions from both attackers and defenders.

B. Explanations of adversarial attack

As large number of parameters and various kinds of structures, to theoretically describe deep learning model is a challenging task. Szegedy et al. first reported adversarial attack and they gave a nonlinear explanation. As deep model has a stack of nonlinear activation functions, i.e. ReLU, TanH, etc, this kind of nonlinearity leads to vulnerability to small perturbation. Szegedy et al. derive a method to generate adversarial examples based on box-constrained L-BFGS. However, this method is an optimization problem and needs plenty of computing resources.

In [20], Goodfellow et al. give a linear explanation. To make further description of linear explanation, firstly we formalize the deep neural network model. In essence, neural network is a kind of mapping function. With different components and architectures, a neural network can "simulate" arbitrary functions. For prevailing application of neural network, image recognition, usually the model is CNN(Convolutional Neural Network). In this case, the model's mapping function is $F: \mathbb{R}^{m \times n} \rightarrow \{0, 1\}^k$. The input of CNN is $m \times n$ image and output is a "one-hot" category vector whose dimension number is k . For example, in ImageNet competition[21], the task is to classify a large amount of images in 1000 categories. Therefore, the mapping function is $F: \mathbb{R}^{227 \times 227} \rightarrow \{0, 1\}^{1000}$.

Without loss of generality, we give the description in binary classification scenario, so $k = 2$. The outputs of the neural network are the probabilities of 2 categories, we note these

2 probabilities as p_1 and p_2 . Usually, the last layer of a classification neural network is softmax layer, so p_1 and p_2 satisfy:

$$p_1 = 1 - p_2 \quad (8)$$

Note input as X , the mapping function of neural network can be written as $F_1(\mathbf{X})$, the subscript of F is the notation of category 1's probability. With (8), we know that $p_1 = F_1(\mathbf{X})$ and $p_2 = 1 - F_1(\mathbf{X})$. To learn the knowledge of training set $\{\mathbf{X}\}$, $F_1(\mathbf{X})$ satisfies that it is differentiable almost everywhere in the input space. We note the gradient matrix of $F_1(\mathbf{X})$ as:

$$\mathbf{G} = \nabla_{\mathbf{X}} F_1(\mathbf{X}) = \begin{bmatrix} \frac{\partial F_1(\mathbf{X})}{\partial X_{1,1}} & \cdots & \frac{\partial F_1(\mathbf{X})}{\partial X_{1,n}} \\ \vdots & \frac{\partial F_1(\mathbf{X})}{\partial X_{i,j}} & \vdots \\ \frac{\partial F_1(\mathbf{X})}{\partial X_{m,1}} & \cdots & \frac{\partial F_1(\mathbf{X})}{\partial X_{m,n}} \end{bmatrix} \quad (9)$$

the element in (i, j) is the gradient value of the pixel X_{ij} . Within a small neighborhood of X_{ij} , $F_1(\mathbf{X})$ is monotonic. When $G_{ij} > 0$, within the local neighborhood of X_{ij} , $F_1(\mathbf{X})$ is increasing. On the contrary, $F_1(\mathbf{X})$ decreases within the local neighborhood when $G_{ij} < 0$. From this we know that, regardless of medium layers and operations of neural network, every element of input data has contribution to the classification result. From (8) we know that:

$$\begin{aligned} \nabla_{\mathbf{X}} p_1 &= \nabla_{\mathbf{X}} F_1(\mathbf{X}) \\ \nabla_{\mathbf{X}} p_2 &= -\nabla_{\mathbf{X}} F_1(\mathbf{X}) \end{aligned} \quad (10)$$

which suggests that p_1 and p_2 changes in opposite direction.

Generally, the basic component of a neural network is neuron, whose math expression can be written as:

$$\mathbf{X}_l = \text{activate}(\mathbf{W}_l \mathbf{X}_{l-1} + \mathbf{b}_l) \quad (11)$$

In (11), notation *activate* is nonlinear activation function. \mathbf{X}_{l-1} is the output of former layer. \mathbf{W}_l and \mathbf{b}_l is the parameter and bias of current layer, respectively. \mathbf{X}_l is the output of current layer. Despite activation function, we know that the basic operation of neuron is linear operation. Therefore, to a great extent, the neural network is based on linear operations.

We construct the adversarial example by adding perturbation to the raw input. Note the perturbation as $\boldsymbol{\eta}$:

$$\tilde{\mathbf{X}} = \mathbf{X} + \boldsymbol{\eta} \quad (12)$$

Consider the operation in neuron:

$$\mathbf{W} \tilde{\mathbf{X}} = \mathbf{W} \mathbf{X} + \mathbf{W} \boldsymbol{\eta} \quad (13)$$

Assume that every element in $\boldsymbol{\eta}$ is a constant C , the activation will raise up by Cmn . The input of neural network is high-dimensional data, i.e., digital image, so mn is sufficiently large enough to remarkably influence the output of neural network.

C. FGS method

From (13) we know that neural network is sensitive to the input perturbation, but it should be emphasized that not any perturbation can inference the output, for example, CNN is robust to random noise. The available perturbation is able to make the output result tend to the constructor's expectation.

Thanks to neural network "end-to-end" architecture, the essential perturbation to generate adversarial example can be derived from gradient.

The back-propagation algorithm is a tool for solving out the derivatives of target function, especially in computational graph. The common application of back-propagation algorithm is training the neural network model. In this case, the task is updating the parameters of network model. The back-propagation algorithm is based on chain-rule, so it can solve out every variable's derivative in the network model. Therefore, besides parameters of each neuron, it can solve out the derivatives of data of each neuron. It is possible to "trace back" the output from last layer to the first layer via back-propagation algorithm, so we can get any target function's derivative of input data. In the training phase of neural network model, the optimizing target is loss function. Loss function reflects the error between the model's output and input data's label(expected output). We note the loss function as $J(\mathbf{X}, y, \theta)$. Fig. 1 demonstrates the typical process of forward-propagation and back-propagation. The forward-

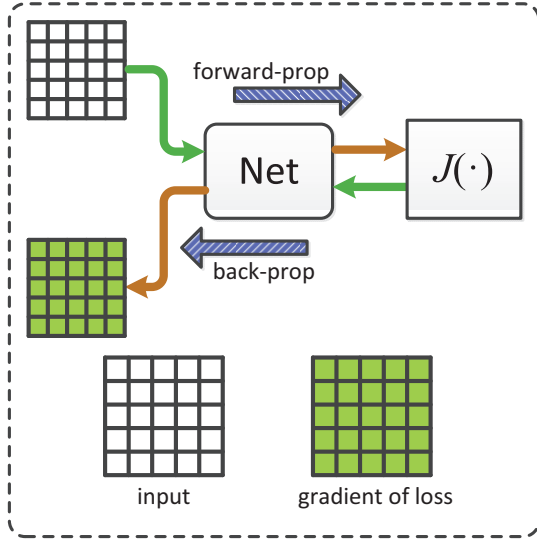


Fig. 1. The typical process of forward-propagation and back-propagation. The purpose is to get the gradient map $\nabla_{\mathbf{X}}J(\mathbf{X}, y, \theta)$.

propagation is computing $J(\mathbf{X}, y, \theta)$ and the back-propagation is computing $\nabla_{\mathbf{X}}J(\mathbf{X}, y, \theta)$.

As $J(\mathbf{X}, y, \theta)$ reflects the error of real output and target, if we need a false category(\tilde{y}), the loss function $J(\mathbf{X}, \tilde{y}, \theta)$ measures the distance to the \tilde{y} . As described in (9), all the element of input data share the contribution to the output result. Therefore, the perturbation η is $\nabla_{\mathbf{X}}J(\mathbf{X}, \tilde{y}, \theta)$. For a digital image, the value type of its pixels is not float but 8-bit integer, in most cases. Therefore, η should be quantified to a proper integer. The dynamic range of 8-bit integer is $\{0, \dots, 255\}$ and value of $\nabla_{\mathbf{X}}J(\mathbf{X}, \tilde{y}, \theta)$ is small (often $< 10^{-8}$), so we use sign function for quantification. The perturbation η generates via FGS method is:

$$\eta = \text{sign}(\nabla_{\mathbf{X}}J(\mathbf{X}, \tilde{y}, \theta)) \quad (14)$$

In practical scenario, the architecture of neural network in training phase has a difference with it in testing phase. That is

in training process, the network model needs loss function to update the parameters, but loss function is unnecessary in testing. The output of a trained network is the category vector or the probability vector of categories. For example, in Caffe[22], during testing phase, the output of network is the probability vector of categories. In this case, we can alter the loss function $J(\cdot)$ to mapping function $F(\cdot)$, so the perturbation is:

$$\eta = \text{sign}(\nabla_{\mathbf{X}}F(\mathbf{X})|_{p=\tilde{p}}) \quad (15)$$

Here, $F(\mathbf{X})|_{p=\tilde{p}}$ means that after forward-propagation (computing $F(\mathbf{X})$), changing the actual result of $F(\mathbf{X})$ to expected value($[\tilde{p}, 1 - \tilde{p}]$). This alternation shares the same effect to $J(\cdot)$, because its goal is to get the changing potential of \mathbf{X} but not the actual value. Fig. (2) shows an example of this alternation. In Fig. (2), after forward

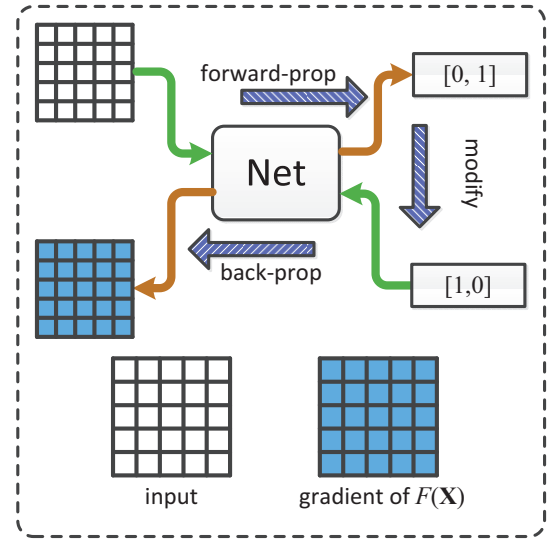


Fig. 2. Replace $J(\cdot)$ with $F(\cdot)$. To generate the perturbation gradient map with a changed category. The gradient map is $\nabla_{\mathbf{X}}F(\mathbf{X})|_{[1,0]}$

propagation, the output vector $[p_1, p_2] = [0, 1]$ is modified to $[\tilde{p}_1, \tilde{p}_2] = [1, 0]$, then conducting back propagation. Setting the softmax probability vector to $[1, 0]$ is equivalent to

D. Generalization

[19][20] reports that adversarial example is not restricted to the neural network model who generates it. For an adversarial example, it is available to a variety kinds of network models and even to feature-based classifying model. Such fact reflects that adversarial example captures the common nature of different classifier models. Attacker can commit adversarial attack without knowing the inner structure of target model. Therefore, a trained network model can be used as a generator for adversarial attack. This new application broadens the task of neural network.

IV. STEGANOGRAPHIC ADVERSARIAL ATTACK

Since first proposal of deep learning based steganalysis, the combination of deep learning and steganalysis has been

a mainstream of relevant research. With deep learning based steganalysis methods, we can enhance the security of existing steganographic methods via adversarial method. However, the adversarial attack is deceiving method, which cannot be applied in steganography directly. To enhance the security of steganographic schemes, it needs adaptation. In this section, we will introduce the adaptation.

A. The weakness of deceiving method

The adversarial attack is deceiving attack, that is exploiting the target's property to get a false classifying result. Such method is effective in deceiving a steganalyzer trained with non-adversarial examples, but cannot confuse the steganalyzer trained with adversarial examples generated by itself. Here we use two simple experiments to show these two capabilities of adversarial examples. The first is to show its deceiving capability, the second is to show its confusing capability.

Consider single-layered STC (SL-STC), which embeds the secret message with LSB replacement (LSBR) method. LSBR alters the LSB of pixel to be modified with secret binary bit. SL-STC only decides the pixels to be modified but not directions of modification (± 1). To get adversarial example via SL-STC, we can decide the modification mode of each pixel (flipping direction) with adversarial perturbation map (η). The map is generated from a trained CNN steganalytic model. The model's training samples are generated with non-adversarial SL-STC. The process of generating the adversarial example is described in Algorithm 1.

Algorithm 1 Generating adversarial examples with SL-STC

Require: \mathbf{X} : cover image

\mathbf{m} : secret message

$F(\cdot)$: neural network (adversarial gradient map generator)

$D(\cdot)$: distortion function

$Emb(\cdot, \cdot, \cdot)$: SL-STC

Ensure: \mathbf{Y} : stego image

- 1: calculate gradient map \mathbf{G} of $F(\mathbf{X})$;
 - 2: embed message $\mathbf{Y} = Emb(\mathbf{X}, D(\mathbf{X}), \mathbf{m})$;
 - 3: find out the changed pixels $\mathbf{Y} - \mathbf{X}$;
 - 4: flip the changed pixels in \mathbf{Y} according to \mathbf{G} ;
 - 5: **return** \mathbf{Y} ;
-

In Fig. 3, we show the key operation of Algorithm 1, which is flipping the changed pixels of stego image. The gray points in the top-left map are the positions of pixels to be changed. In adversarial perturbation map (top-right), red point and blue point is $+1$ and -1 , respectively. These two maps determined the final output.

The first experiment is demonstration of adversarial attack. The distortion function is S-UNIWARD. We randomly select 5000 cover images from BOSSbase as training set, other 5000 cover images as testing set. The gradient map generator is XuNet trained with default super parameters proposed in [15]. We will train 5 gradient map generators in 5 payload rates (0.05, 0.1, 0.2, 0.3, 0.4). The training samples of XuNet are generated by non-adversarial SL-STC in 5 payload rates. The target steganalyzer of adversarial attack are 5 maxSRM

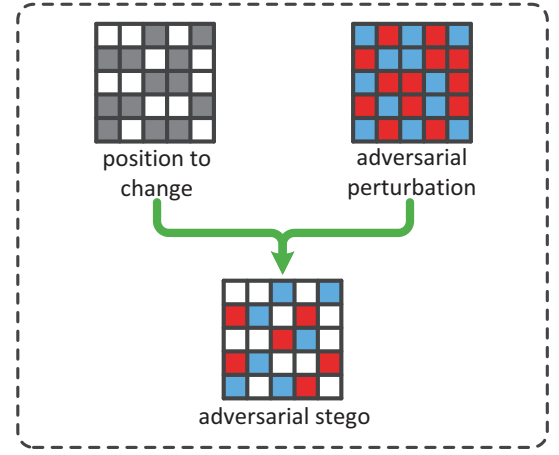


Fig. 3. Determining the flipping directions according to $sign(\mathbf{G})$. Top-left: gray points are the pixels to be changed. Top-right: adversarial perturbation sign map, red point is $+1$ and blue point is -1 . Bottom: the generated adversarial stego image.

+ ensemble classifiers, whose training sets are the same as gradient map generators in 5 payload rates. The rest 5000 images are for testing. Under each payload rate, We generate the adversarial example from covers via Algorithm 1. Then we use them to attack(test) the steganalyzer in the corresponding payload rate. We note the first experiment as "Exp I".

In second experiment, we will test the steganographic security of adversarial examples with P_E metric. We generate adversarial examples in 5 payload rates from the testing cover set (5000 images). The gradient map generators are 5 generators used in the first experiment. Under each payload rate, we use 2500 cover/adversarial stego pairs to train the steganalyzer and other 2500 pairs to test. We note the second experiment as "Exp II".

The main difference between Exp I and Exp II is that in Exp I, the being attacked steganalyzers' training sets are non-adversarial while in Exp II, the being attacked steganalyzers' training sets are adversarial.

The results are shown in Fig. 4. In the figure there are also testing results of non-adversarial SL-STC + SUNIWARD towards maxSRM[23]. It is the baseline that reflects the security of typical adaptive steganographic scheme.

From Fig. 4 we can see that P_E s of Exp I are around 50%, which means that adversarial example can effectively deceive the steganalyzer. However we can also see that P_E s are significantly decreased in Exp II. The result of Exp II implies that adversarial example cannot improve the security of steganographic schemes. Comparing with common adaptive steganography, the method used in Exp II is not secure.

B. Confusing the steganalyzer

To generate adversarial perturbation map, the typical adversarial method example is setting the output to a false category. As output of softmax $[p_c, p_s]$ can be set arbitrarily, we improve the typical adversarial method by set $[p_c, p_s]$ to an arbitrary vector rather than $[1, 0]$. We find that when $[p_c, p_s]$ is set to $[0.5, 0.5]$, the gradient map can substantially

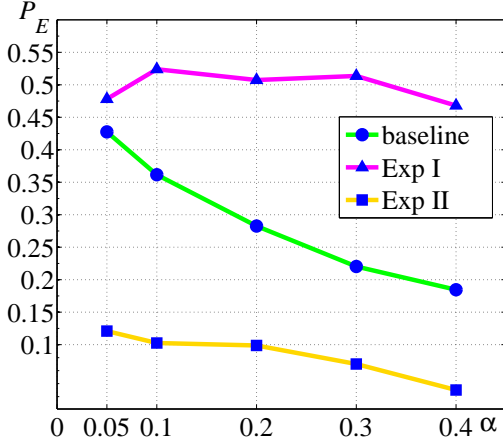


Fig. 4. Results of Exp I and Exp II. Exp I is testing the adversarial stego images by steganalyzer trained with non-adversarial stego images. Exp II is testing the adversarial stego images by steganalyzer trained with adversarial stego images. The "baseline" is testing the non-adversarial stego images by steganalyzer trained with non-adversarial stego images, which is for comparing.

improve the performance of steganographic scheme towards the steganalyzer trained with adversarial examples. In this section, we discuss this improvement.

Adversarial example exploits the characteristic of classifier, it can deceive the classifier effectively. The typical process to generate adversarial gradient map is setting the network's output category vector to a false result, and then conducting back-propagation. This process is equivalent to setting the softmax layer's output to a one-hot vector, which means that the target category's probability is 1 and others' are 0. For example, the output of softmax layer in steganalytic neural network is $[p_c, p_s]$. To generate adversarial example, $[p_c, p_s]$ is set to $[1, 0]$, to make sure that stego image is misclassified to cover image.

Consider the element of gradient map $\mathbf{G} = \nabla_{\mathbf{X}} F(\mathbf{X})$, G_{ij} , which reflects the potential of changing. We note that the output of steganalyzer is $[p_c, p_s]$, p_c is the probability of cover and p_s is the probability of stego. When the output is set, $F(\mathbf{X})|_{[p_c, p_s]}$, then G_{ij} is the error metric of X_{ij} to the target output $[p_c, p_s]$. To train the model, the gradient decent algorithm updates the parameters of the model to reach the target. On the other hand, from (11) we know that \mathbf{W} and \mathbf{X} have the same contributions to the output. Therefore, without update parameters, it also effective to modify \mathbf{X} with \mathbf{G} to pursue the target output.

In essence, the adversarial method enlarges the "distance" between the generated samples and the cover samples, comparing with non-adversarial samples. Note the input space of the network model as \mathbb{S} . All the input samples are points in \mathbb{S} . Note that in \mathbb{S} , cover instance is \mathbf{X} , non-adversarial stego instance is \mathbf{Y}_{non} , adversarial stego instance is \mathbf{Y}_{adv} . The typical stego embedding operation generate \mathbf{Y}_{non} from \mathbf{X} .

The adversarial attack can deceive the models which are trained with non-adversarial samples. The network model is a hyperplane in \mathbb{S} and divides the space into several parts

according to the categories. In steganalysis, the task is to classify stego images and cover images. For a well-trained steganalyzer, it can discriminate \mathbf{Y}_{non} and \mathbf{X} correctly. \mathbf{Y}_{adv} is generated with the network model. The target of \mathbf{Y}_{adv} is deceiving the classifiers shares similarities with its generator. Intuitively, The steganographic security of \mathbf{Y} is highly related to its "distance" to \mathbf{X} . \mathbf{Y}_{adv} is located in the cover space. To deceive the steganalyzer effectively, it is deviated from the hyperplane of its generator to a maximum extent. However, this operation also increases the distance between \mathbf{X} and \mathbf{Y}_{adv} . Therefore, \mathbf{Y}_{adv} is more distinguishable than \mathbf{Y}_{non} and can be detected more easily than \mathbf{Y}_{non} .

To be less distinguishable, we need to generate a sample that close to \mathbf{X} via adversarial method. We name this sample as "confusing sample" and note it as \mathbf{Y}_{con} . Fig. 5 depicts the \mathbb{S} . In the figure, we can see that $d_{con} < d_{non}$ and $d_{con} < d_{adv}$. Our task is to design a method to generate \mathbf{Y}_{con} .

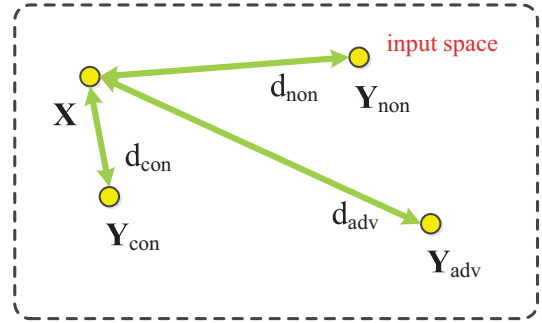


Fig. 5. Different kinds of samples in \mathbb{S} . \mathbf{X} is cover sample. \mathbf{Y}_{non} is common non-adversarial stego sample. \mathbf{Y}_{adv} is adversarial stego sample generated via $\nabla_{\mathbf{X}} F(\mathbf{X})|_{[1,0]}$. \mathbf{Y}_{con} is the adversarial sample that we need to find. d_{non} , d_{adv} , and d_{con} are their distance to sample \mathbf{X} , respectively.

The ideal case to confuse the steganalyzer is locating \mathbf{Y}_{con} on \mathbf{X} , which is hard to implement. Therefore, we need to make \mathbf{Y}_{con} close to \mathbf{X} . We can add an interference to the input. Consider the case that $[p_c, p_s]$ is set to $[0.5, 0.5]$, $F(\mathbf{Y}_{con}) = 0.5 = p_c = 1 - p_s$. This is the case that steganalyzer can not discriminate the category of the input. The generated gradient map under this case is the perturbation map we need:

$$\eta = \text{sign}(\nabla_{\mathbf{X}} F(\mathbf{X})|_{p=0.5}) \quad (16)$$

MMD[24] is a metric of distance in feature space. Here we use MMD to measure 3 kinds of samples' distance to cover samples, which are: non-adversarial samples(A); adversarial samples, $[p_c, p_s] = [1, 0]$ (B), and adversarial samples, $[p_c, p_s] = [0.5, 0.5]$ (C). We randomly choose 100 images from BOSSbase. The distortion function S-UNIWARD, and payload rate is 0.4. The steganalytic feature is SPAM[25]. Table I shows the result. From Table I we can see that type C, corresponding adversarial samples and $[p_c, p_s] = [0.5, 0.5]$, has lowest MMD. Type B, corresponding adversarial samples and $[p_c, p_s] = [1, 0]$, has highest MMD. Therefore, type C has the lowest distance.

Now we testing the performance of alternative method. We note this experiment as "Exp III". The experiment setting is the same as Exp II in Section IV-A, the difference is that the method to generate perturbation map is (16). Fig. 6 shows the

TABLE I
MMD OF 3 KINDS OF SAMPLE

Sample Type	MMD
A	5.979×10^{-33}
B	7.774×10^{-33}
C	2.415×10^{-33}

result. We can see that the improved method performs better

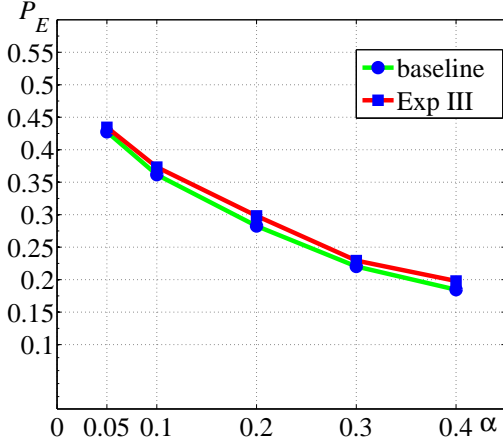


Fig. 6. Results of Exp III. The adversarial stego images is generated with the improved method(16). The steganalyzer is trained with the same kind of adversarial images. The "baseline" is the same as Fig. 4.

than the baseline. Therefore, the alternative method is effective to improve the security of steganographic schemes.

V. PRACTICAL ADVERSARIAL STEGANOGRAPHIC SCHEME

In the last section, we discuss the adaptation of adversarial attack to steganography. We adopt a simple adversarial method based on SL-STC to improve the security of typical adaptive steganographic algorithm. However, SL-STC based method cannot utilize ± 1 to embed more information, which leads to low efficiency.

In this section, we employ the adversarial method to improve double-layered STC(DL-STC). The implemented method is generally based on distortion updating, which makes cost value of $+1$ not equal to cost value of -1 . With the distortion updating, the framework of the proposed method can be flexible to different kinds of distortion functions and multi-layered STC.

We first describe the general implementation of the scheme. Secondly we discuss the detail designs and parameters. Finally, we visualize the embedding effects of the proposed scheme. Note that the proposed method is not limited to specific distortion function.

A. General implementation

We first introduce the general operations of generating stego adversarial examples with DL-STC. In Algorithm 2, ρ represents the distortion map for DL-STC, which is a 3-ary matrix. In ρ , $\rho_{ij} = \{\rho_{ij}^+, \rho_{ij}^0, \rho_{ij}^-\}$. We can see that the

Algorithm 2 Generating adversarial examples with DL-STC

Require: \mathbf{X} : cover image

\mathbf{m} : secret message

$F(\cdot)$: neural network (adversarial gradient map generator)

$D(\cdot)$: distortion function

$Emb(\cdot, \cdot, \cdot)$: DL-STC

Ensure: \mathbf{Y} : stego image

- 1: calculate gradient map \mathbf{G} of $F(\mathbf{X})$ by(16);
- 2: calculate distortion map $\rho = D(\mathbf{X})$;
- 3: update ρ to ρ' with \mathbf{G} ;
- 4: embed message $\mathbf{Y} = Emb(\mathbf{X}, \rho', \mathbf{m})$
- 5: **return** \mathbf{Y} ;

important operation is updating the distortion map ρ with adversarial gradient map \mathbf{G} .

The key to employ adversarial attack is controlling $+1$ or -1 of pixels. The similar idea also appears in SMD strategy. In SMD, the mutual embedding effect of local pixels is considered. To control $+1$ or -1 in DL-STC, SMD applies the distortion updating principle. As $\rho^+ \neq \rho^-$, the corresponding pixel can be modified with expectation during embedding.

We also apply distortion updating principle to generate steganographic adversarial example using DL-STC. The principle used in SMD only updates the cost value by multiplying or dividing a constant. In our implementation, we take a further step. Besides the gradient's sign, we also update the cost considering the gradient's value. For a pixel X_{ij} , its cost values are noted as ρ_{ij}^* , here $*$ $\in \{+, -\}$. We also get its gradient G_{ij} with (16). The updated cost values are:

$$\begin{cases} \rho_{ij}' = A(G_{ij}) \times \rho_{ij}^*, & \text{if } * = \text{sign}(G_{ij}) \\ \rho_{ij}' = \rho_{ij}^*, & \text{if } * \neq \text{sign}(G_{ij}). \end{cases} \quad (17)$$

$A(G_{ij})$ is a scaling parameter which is determined by G_{ij} , satisfies $1 < \|G_{ij}\| < 0$. We only change the cost value whose sign is the same as G_{ij} 's. Other details of $A(G_{ij})$ will be discussed later. With cost updating, we can control the flipping directions of embedding changes. Fig. 7 shows the cost updating operation.

B. Detail design

We first discuss the design of $A(G_{ij})$. $A(G_{ij})$ is for scaling operation. Different choice of $A(G_{ij})$ will introduce different effect to the stego image. Given a distortion function, the profile of each pixel's cost value is determined. DL-STC will follow these profiles to change the pixels. When introduce distortion updating to the distortion map, the cost values are changed. This operation can bring more diversities to the distortion function. Here we propose 2 designs of $A(G_{ij})$. Updating function I is a linear function. Its expression is:

$$A(G_{ij}) = 1 - \frac{1}{2}\|G_{ij}\| \quad (18)$$

Updating function II is a non-linear function. Its expression is:

$$A(G_{ij}) = \frac{1}{1 + \|G_{ij}\|} \quad (19)$$

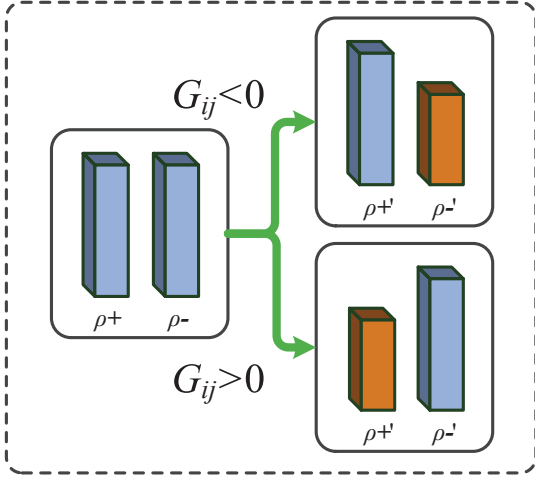


Fig. 7. Cost updating operation. There are 3 blocks. In each block, the pillar on left is ρ^+ and the pillar on right is ρ^- . We only update the ρ whose sign is the same as G_{ij} and make it smaller than another ρ .

Different choice of $A(G_{ij})$ introduces different effect to the distortion function.

The second detail is the amplification of gradient map \mathbf{G} . The generator used here is optimized neural network model. The parameter of the generator tend to be steady in the training process, which suggests that the gradients of parameters and feature maps tend to be small. Therefore, the value of \mathbf{G} 's element is not significant. We choose "1013.pgm" from BOSSbase. We calculate its gradient map \mathbf{G} on XuNet. We find that the max value of \mathbf{G} is 1.4×10^{-11} .

Comparing with cost value ρ_{ij} of pixel X_{ij} , the gradient G_{ij} is negligible. To make sure that $A(G_{ij})$ has a significant impact, we amplify \mathbf{G} :

$$\mathbf{G}' = \frac{1}{\max(\mathbf{G})} \mathbf{G} \quad (20)$$

Function $\max(\cdot)$ represents finding out the maximum value. As $\max(G_{ij}) \ll 10^0$, \mathbf{G}' satisfy $\|\mathbf{G}'_{ij}\| \gg \|G_{ij}\|$. So \mathbf{G} can influence the cost values more significantly.

The third detail design is removing chessboard pattern of $\text{sign}(\mathbf{G})$. In practical scenario we find that $\text{sign}(\mathbf{G})$ has chessboard pattern(+1 and -1 appearing regularly) in the smooth area of \mathbf{X} . Here is an example to demonstrate the chessboard pattern. We choose "1.pgm" from BOSSbase. Fig. 8 shows its $\text{sign}(\mathbf{G})$ calculated via XuNet model. In Fig. 8, the

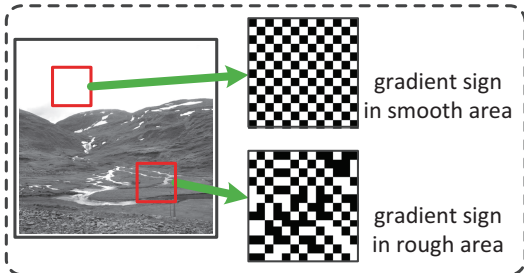


Fig. 8. Chessboard pattern of $\text{sign}(\mathbf{G})$. The chessboard pattern only exists in the smooth area of the image. In rough area, the pattern of $\text{sign}(\mathbf{G})$ is irregular.

black point in $\text{sign}(\mathbf{G})$ implies -1 and white point implies +1. We can see that the gradient sign map $\text{sign}(\mathbf{G})$ has chessboard pattern in smooth area of the image. On the contrary, in rough area of the image, $\text{sign}(\mathbf{G})$ has irregular pattern. $\text{sign}(\mathbf{G})$ suggests the flipping directions of the pixels. In steganalysis, the typical detector utilizes the filters to capture specific local modification patterns. Therefore, flipping the pixels following chessboard pattern will make the stego image vulnerable to the steganalysis. We need to remove the chessboard pattern of $\text{sign}(\mathbf{G})$.

We use a mask to match the chessboard pattern and remove it. Consider the matrix:

$$\mathbf{T} = \begin{bmatrix} -1 & 1 & -1 \\ 1 & -1 & 1 \\ -1 & 1 & -1 \end{bmatrix} \quad (21)$$

It is the mask for matching the pattern. We match the chessboard pattern with cross-correlation operation:

$$\mathbf{K} = \text{sign}(\mathbf{G}) \odot \mathbf{T} \quad (22)$$

In (22), operator \odot is cross-correlation. Please be aware of the difference between convolution and cross-correlation. With the cross-correlation map \mathbf{K} , we can remove the chessboard pattern as follows. For every (i, j) :

$$G_{ij} = 0, \text{ if } \|K_{ij}\| = 9 \quad (23)$$

$\|K_{ij}\| = 9$ matches the pattern \mathbf{T} and pattern $-\mathbf{T}$. When $G_{ij} = 0$, so $\text{sign}(G_{ij}) = 0$, then the flipping direction of X_{ij} does not have bias and is chosen randomly by DL-STC.

We visualize this operation in Fig. 9. We can see that the

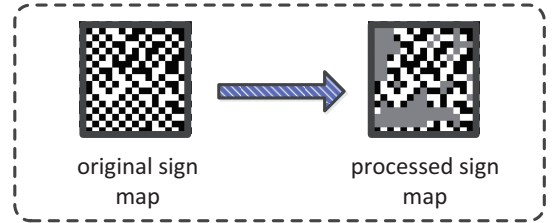


Fig. 9. Removing the chessboard pattern. We remove the chessboard pattern by (22). The gray area is removed-pattern area. In the gray area, $G_{ij} = 0$.

original sign map has chessboard pattern. In the processed sign map, the chessboard pattern is removed. The gray point in the sign map implies 0, which is the point located in the removed chessboard area.

C. Visualization

In this section, we visualize the embedding result of proposed method. Fig. 10 shows the embedding result. We choose a portion of "1013.pgm" in BOSSbase to show the result. We embed a random payload in payload rate 0.4 and with distortion function S-UNIWARD. We can see that nearly all the modified pixels follow the gradient sign map.

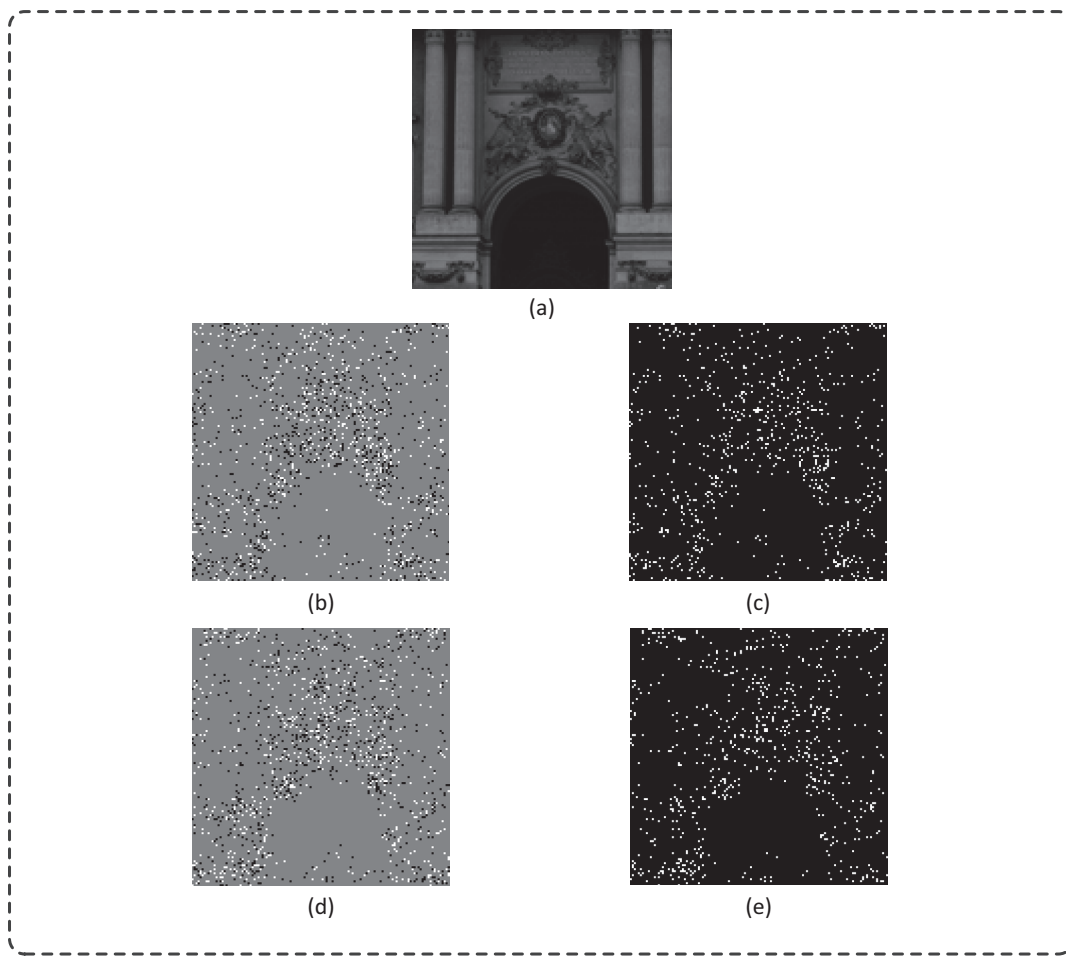


Fig. 10. Visualization of proposed method. (a) is the portion of cover image. (b) is modification pattern of S-UNIWARD combined with updating function I(18), white points are $+1$ and black points are -1 . (c) shows the pixels in (b) that follows the gradient sign. (d) and (e) is the same as (b) and (c), respectively, but the distortion function is updated with updating function II(19).

VI. EXPERIMENT

In this section, we will test the performance of the proposed method. We first test the adversarial method with rich-model based steganalyzer. Then we test the method with steganalytic neural network. The type of perturbation gradient map generator is XuNet. We apply 3 distortion functions: S-UNIWARD, HILL, and MIPOD. The chosen payload rates are 0.05, 0.1, 0.2, 0.3, 0.4.

A. Rich model steganalysis

The testing steganalyzer are SRM + ensemble classifier[26] and maxSRM + ensemble classifier. The image set is the mixture of BOSSbase and BOWSbase, which includes 20000 images totally. We randomly choose 10000 images from the set to train the generators and the other 10000 images are for testing. Having chosen a distortion function and a payload rate, we generate 10000 stego images with non-adversarial method. Then we train a generator with 10000 cover/stego pairs. We use the default super-parameters proposed in [15].

With a generator in particular distortion function and payload rate, we generate the steganographic adversarial samples using the rest 10000 images. Then we test their performance

to resist the detecting of steganalyzer with '5000/5000' manner, which is choosing 5000 cover/stego pairs to train the steganalyzer and another 5000 pairs for testing. We use P_E to evaluate the performance.

For convenience, we use abbreviation of distortion function to note the results of non-adversarial methods: "SUNI" for S-UNIWARD, "MIPO" for MIPOD, and "HILL" for HILL. SUNI, MIPO, and HILL are for comparing. We also use abbreviation to note the adversarial method. The notation is the combination of distortion function name and updating function type. For example, S-UNIWARD with updating function I, we note it as "SUNI-I"; MIPOD with updating function II, we note it as "MIPO-II". Fig. 11 shows the results. In the result we know that proposed adversarial steganographic scheme can improve the performance of original steganographic schemes.

B. Neural network steganalysis

In section VI-A, we test the proposed method with rich model. In this section, we test the proposed method with steganalytic neural network. As XuNet has good performance and is suitable for 512×512 image, we still choose XuNet as steganalyzer.

TABLE II
EXPERIMENT RESULTS ON XUNET

method	HILL-I	HILL	SUNI-I	SUNI	MIPO-I	MIPO
P_E	0.2822	0.2334	0.2735	0.2082	0.3159	0.2409

From the experiment results of section VI-A (Fig. 11) we find that methods equipped with updating function I has better performance than updating function II. We will test the performance of HILL-I, SUNI-I, and MIPO-I, under payload rate 0.4. For each method, we generate 10000 stego images. We train the steganalyzer with 5000 cover/stego pairs, and the other 5000 pairs for testing. The super-parameters of training XuNet is also the default setting.

Table II shows the experiment results. We can see that P_E s of adversarial methods are larger than non-adversarial methods'. These results prove that the proposed adversarial method is also effective to enhance the security towards the deep-learning based steganalysis.

VII. CONCLUSION

In this paper, we propose an application of adversarial method in steganography. The proposed method is proved to be effective to improve the steganographic security of typical spatial adaptive steganographic methods. The proposed method is derived from FGS method and is combined with distortion-minimizing steganography. In contrast to the intuitive goal of adversarial attack, which is to make the input misclassified, we adjust our method to improve the steganographic security of existing methods. Essentially, with the adversarial method, we make the stego images more undistinguishable from cover images comparing with typical steganographic methods. We adopt the proposed method to HILL, S-UNIWARD, and MIPOD. The experiment results prove that the proposed method is effective to resist the rich-model based steganalysis and deep-learning based steganalysis.

Our method is a practical method to improve the performance of existing steganographic scheme. Firstly, its requirement is acceptable. For an typical adaptive steganographic system, to use the proposed method, the additional requirement is a neural network model. Secondly, the proposed method is flexible. It can be combined with the existing adaptive steganographic methods. In this paper we use it to improve the spatial methods. With some modification, it can be also applied in JPEG steganographic methods. Thirdly, the complexity is tolerable. Comparing with typical schemes, to generate a adversarial stego image, the additional operations are: 1 forward-propagation on generator, 1 back-propagation on generator, and 1 cost updating operation.

Furthermore, the adversarial process on neural network can be iterative, which means using the adversarial examples to train another network model and repeating this process. In the future work, we will explore the iterative adversarial method.

ACKNOWLEDGMENT

The authors would like to thank the members of DDE Laboratory in SUNY Binghamton for sharing their codes

and image base, and the members of MICS Laboratory in Shenzhen University for sharing their codes. The authors would also like to thank the authors of Caffe.

REFERENCES

- [1] T. Filler, J. Judas, and J. Fridrich, "Minimizing additive distortion in steganography using syndrome-trellis codes," *IEEE Transactions on Information Forensics and Security*, vol. 6, no. 3, pp. 920–935, Sept 2011.
- [2] T. Pevny, T. Filler, and P. Bas, "Using high-dimensional image models to perform highly undetectable steganography," in *International Workshop on Information Hiding*. Springer, 2010, pp. 161–177.
- [3] V. Holub and J. Fridrich, "Designing steganographic distortion using directional filters," in *2012 IEEE International Workshop on Information Forensics and Security (WIFS)*, Dec 2012, pp. 234–239.
- [4] V. Holub and J. Fridrich, "Digital image steganography using universal distortion," in *Proceedings of the first ACM workshop on Information hiding and multimedia security*. ACM, 2013, pp. 59–68.
- [5] B. Li, M. Wang, J. Huang, and X. Li, "A new cost function for spatial image steganography," in *2014 IEEE International Conference on Image Processing (ICIP)*, Oct 2014, pp. 4206–4210.
- [6] B. Li, S. Tan, M. Wang, and J. Huang, "Investigation on cost assignment in spatial image steganography," *IEEE Transactions on Information Forensics and Security*, vol. 9, no. 8, pp. 1264–1277, Aug 2014.
- [7] J. Fridrich and J. Kodovsky, "Multivariate gaussian model for designing additive distortion for steganography," in *2013 IEEE International Conference on Acoustics, Speech and Signal Processing*, May 2013, pp. 2949–2953.
- [8] V. Sedighi, R. Cogranne, and J. Fridrich, "Content-adaptive steganography by minimizing statistical detectability," *IEEE Transactions on Information Forensics and Security*, vol. 11, no. 2, pp. 221–234, Feb 2016.
- [9] B. Li, M. Wang, X. Li, S. Tan, and J. Huang, "A strategy of clustering modification directions in spatial image steganography," *IEEE Transactions on Information Forensics and Security*, vol. 10, no. 9, pp. 1905–1917, Sept 2015.
- [10] T. Denemark and J. Fridrich, "Improving steganographic security by synchronizing the selection channel," in *Proceedings of the 3rd ACM Workshop on Information Hiding and Multimedia Security*, ser. IH&MMSec '15. New York, NY, USA: ACM, 2015, pp. 5–14.
- [11] W. Zhang, Z. Zhang, L. Zhang, H. Li, and N. Yu, "Decomposing joint distortion for adaptive steganography," *IEEE Transactions on Circuits and Systems for Video Technology*, vol. 27, no. 10, pp. 2274–2280, Oct 2017.
- [12] S. Tan and B. Li, "Stacked convolutional auto-encoders for steganalysis of digital images," in *Signal and Information Processing Association Annual Summit and Conference (APSIPA)*, 2014 Asia-Pacific, Dec 2014, pp. 1–4.
- [13] J. Fridrich and J. Kodovsky, "Rich models for steganalysis of digital images," *IEEE Transactions on Information Forensics and Security*, vol. 7, no. 3, pp. 868–882, June 2012.
- [14] Y. Qian, J. Dong, W. Wang, and T. Tan, "Deep learning for steganalysis via convolutional neural networks," in *SPIE/IS&T Electronic Imaging*. International Society for Optics and Photonics, 2015, pp. 94 090J–94 090J.
- [15] G. Xu, H. Z. Wu, and Y. Q. Shi, "Structural design of convolutional neural networks for steganalysis," *IEEE Signal Processing Letters*, vol. 23, no. 5, pp. 708–712, May 2016.
- [16] J. Ye, J. Ni, and Y. Yi, "Deep learning hierarchical representations for image steganalysis," *IEEE Transactions on Information Forensics and Security*, vol. 12, no. 11, pp. 2545–2557, Nov 2017.
- [17] D. Volkhonskiy, I. Nazarov, B. Borisenko, and E. Burnaev, "Steganographic generative adversarial networks," *arXiv preprint arXiv:1703.05502*, 2017.
- [18] W. Tang, S. Tan, B. Li, and J. Huang, "Automatic steganographic distortion learning using a generative adversarial network," *IEEE Signal Processing Letters*, vol. 24, no. 10, pp. 1547–1551, Oct 2017.
- [19] C. Szegedy, W. Zaremba, I. Sutskever, J. Bruna, D. Erhan, I. Goodfellow, and R. Fergus, "Intriguing properties of neural networks," *arXiv preprint arXiv:1312.6199*, 2013.
- [20] I. Goodfellow, J. Shlens, and C. Szegedy, "Explaining and harnessing adversarial examples," *arXiv preprint arXiv:1412.6572*, 2014.
- [21] J. Deng, W. Dong, R. Socher, L.-J. Li, K. Li, and L. Fei-Fei, "ImageNet: A Large-Scale Hierarchical Image Database," in *CVPR09*, 2009.

- [22] Y. Jia, E. Shelhamer, J. Donahue, S. Karayev, J. Long, R. Girshick, S. Guadarrama, and T. Darrell, "Caffe: convolutional architecture for fast feature embedding," *arXiv preprint arXiv:1408.5093*, 2014.
- [23] T. Denemark, V. Sedighi, V. Holub, R. Cogranne, and J. Fridrich, "Selection-channel-aware rich model for steganalysis of digital images," in *2014 IEEE International Workshop on Information Forensics and Security (WIFS)*, Dec 2014, pp. 48–53.
- [24] T. Pevny and J. Fridrich, "Benchmarking for steganography," in *International Workshop on Information Hiding*. Springer, 2008, pp. 251–267.
- [25] T. Pevny, P. Bas, and J. Fridrich, "Steganalysis by subtractive pixel adjacency matrix," *IEEE Transactions on Information Forensics and Security*, vol. 5, no. 2, pp. 215–224, June 2010.
- [26] J. Kodovsky, J. Fridrich, and V. Holub, "Ensemble classifiers for steganalysis of digital media," *IEEE Transactions on Information Forensics and Security*, vol. 7, no. 2, pp. 432–444, April 2012.

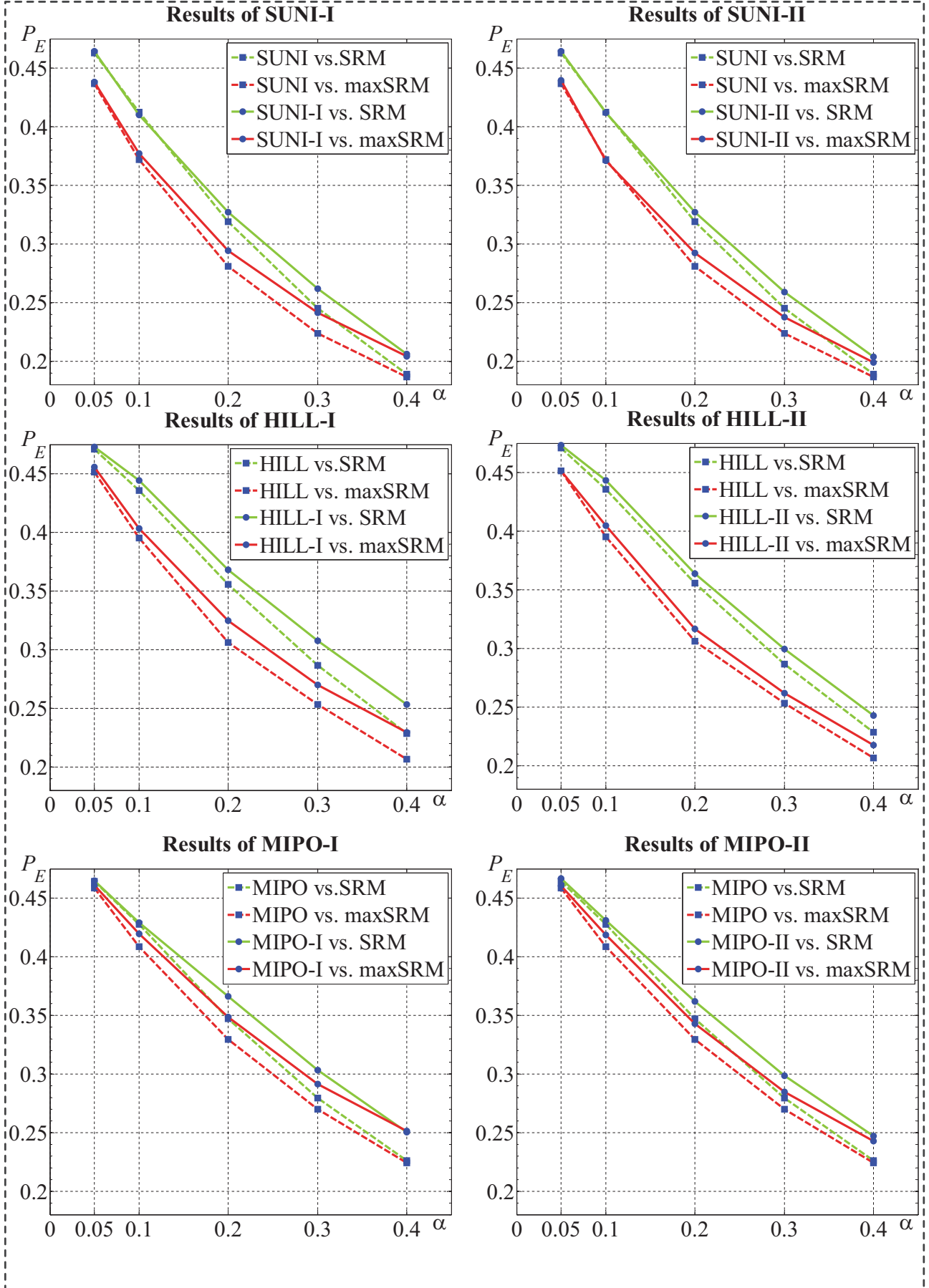


Fig. 11. The experiment results of testing the proposed methods with rich model(SRM and maxSRM)